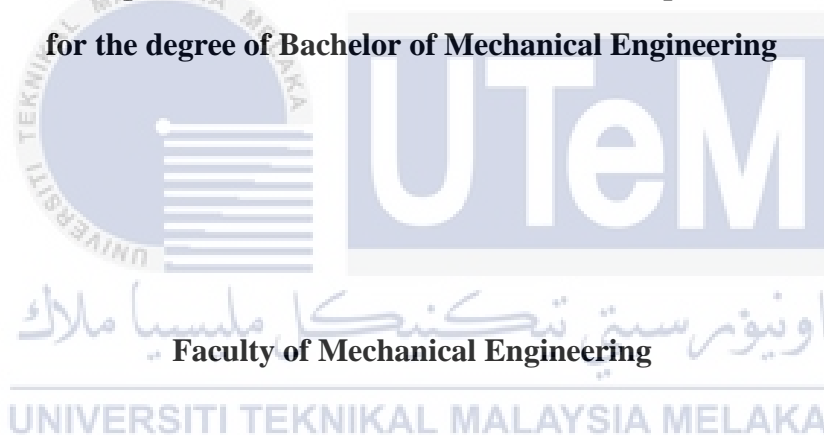


NUMERICAL INVESTIGATION OF NANOFLUID FLOW AND HEAT TRANSFER INSIDE A MICROCHANNEL

MUHAMMAD SYAFIQ BIN MD RADZI

**This report is submitted in fulfilment of the requirement
for the degree of Bachelor of Mechanical Engineering**



UNIVERSITI TEKNIKAL MALAYSIA MELAKA

2018

DECLARATION

I declare that this project report entitled “Numerical investigation of nanofluid flows and heat transfer inside a microchannel” is the result of my own work except as cited in the references

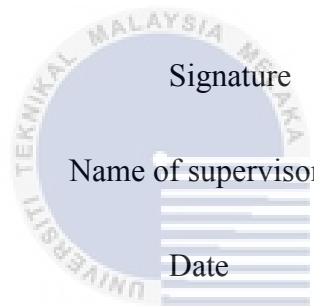
	Signature :	
	Name :	
	Date :	

اونيورسيتي تيكنيكل مليسيا ملاك

UNIVERSITI TEKNIKAL MALAYSIA MELAKA

APPROVAL

I hereby declare that I have read this project and in my opinion this project is sufficient in terms of scope and quality for the award of the degree of Bachelor of Mechanical Engineering (with Honours).

	Signature	:
	Name of supervisor	:
	Date	:

اونيورسيتي تيكنيكل مليسيا ملاك

UNIVERSITI TEKNIKAL MALAYSIA MELAKA

ABSTRACT

Microchannel is widely used in micro-electronics industry from time to time in achieving the lowest thermal resistance equipment. The objectives of this study are to simulate the nanofluid flows with correlation to velocity profiles generated in the study. In this study, nanofluid of alumina, Al_2O_3 with kinematic viscosity of $0.001028 \text{ kg/ms}^{-1}$ is used as the working fluid inside the microchannel. Reynolds number of 140, 300 and 500 are used in configuring nanofluid flows and thermal conductivity of the microchannel. These low Reynolds numbers have developed to very small entrance region of 0.5mm, 2.0mm and 4.0mm with constant laminar and fully developed flow for the nanofluid. Higher Reynolds number results to higher velocity magnitude of 2.36%, 4.47% and 11.63% with constant percentage of increment. The Nusselt number is higher at the channel inlet and became closer to zero as it approached to the corner. Constant temperature gradient is observed throughout the microchannel in transverse y – direction where separation of solid and liquid boundaries is clearly visible.

اونيورسيتي تيكنيكل مليسيا ملاك

UNIVERSITI TEKNIKAL MALAYSIA MELAKA

ABSTRAK

Mikrosaluran banyak digunakan dalam industri mikro-elektronik dalam semasa ke semasa untuk mencapai peralatan tahan panas terendah. Objektif kajian ini adalah untuk mengaplikasi aliran cecair alumina dengan hubungkait pada corak kelajuan yang dihasilkan dalam kajian. Dalam kajian ini, nanofluid alumina, Al_2O_3 dengan kelikatan kinematik $0,001028 \text{ kg/ms}^{-1}$ digunakan sebagai airan kerja di dalam mikrosaluran. Nombor Reynolds 140, 300 dan 500 digunakan dalam mengkonfigurasi aliran nanofluid dan mengesan konduktiviti termal dalam mikrosaluran. Nombor Reynolds yang rendah ini telah menghasilkan panjang kemasukan yang sangat kecil iaitu 0.5 mm, 2.0 mm, dan 4.0 mm dengan aliran yang perlahan dan sama sepanjang mikrosaluran. Hasil Reynolds yang lebih tinggi menghasilkan kelajuan magnitud yang lebih tinggi iaitu 2.36%, 4.47% dan 11.63% dengan peratusan kenaikan yang sama. Nombor Nusselt yang lebih tinggi pada saluran masuk menghampiri kosong pada saluran keluar. Perubahan suhu yang sama dapat dilihat di seluruh mikrosaluran dalam arah y melintang di mana pemisahan batas antara logam dan cecair jelas terlihat.

اوتنورسي تيكنيكل مليسيا ملاك

UNIVERSITI TEKNIKAL MALAYSIA MELAKA

ACKNOWLEDGEMENT

The completion of this Final Year Project could not have been possible without the assistance and participation of many people whose names may not all be written. I am thankful for their aspiring guidance, invaluable constructive criticism and friendly advice during the project work. Their contributions are sincerely appreciated and gratefully acknowledge.

Among others, I would like to express my sincere gratitude to my final year project supervisor, Dr Ernie Binti Mat Tokit, whose contribution in giving encouragement and suggestion, helped me coordinate my project especially in writing this report. I am grateful and honoured to her for all the knowledge, wisdom and experience she shared during my studies.

Finally, it is impossible to name everyone who helped, guided and encouraged me when I am working on my thesis. I take this opportunity to thank all of them especially to my family and friends for their constant understanding and inspiration.

UNIVERSITI TEKNIKAL MALAYSIA MELAKA

Contents

ABSTRACT	i
ABSTRAK	ii
ACKNOWLEDGEMENT	iii
LIST OF FIGURES	vi
LIST OF TABLES	vii
LIST OF ABBREVIATIONS	viii
LIST OF SYMBOL	ix
CHAPTER 1	1
Introduction	1
1.1 Background of Study	1
1.2 Problem Statement	3
1.3 Objectives	3
1.4 Scope of Project	3
1.5 General Methodology	4
CHAPTER 2	5
Literature Review	5
2.1 Introduction	5
2.2 Nanofluid Characteristics	5
2.3 Reynolds number and its significance	6
2.4 Factors affecting fluid flow of nanofluid	7
CHAPTER 3	11
Methodology	11
3.1 Introduction	11
3.2 3D Design Domain	13
3.3 3D Modelling Mesh Discretization	13
3.4 Boundary Conditions	15
3.5 Thermal properties	17
CHAPTER 4	18
Results	18
4.1 Introduction	18
4.2 Mesh Independence Test	18
4.3 Validation	20
4.4 Velocity Profile	22
4.5 Local Temperature Distribution	27

4.6	Heat Flux	30
4.7	Nusselt Number	32
CHAPTER 5.....		33
Conclusion.....		33
5.1	Introduction	33
5.2	Conclusion.....	33
References		35

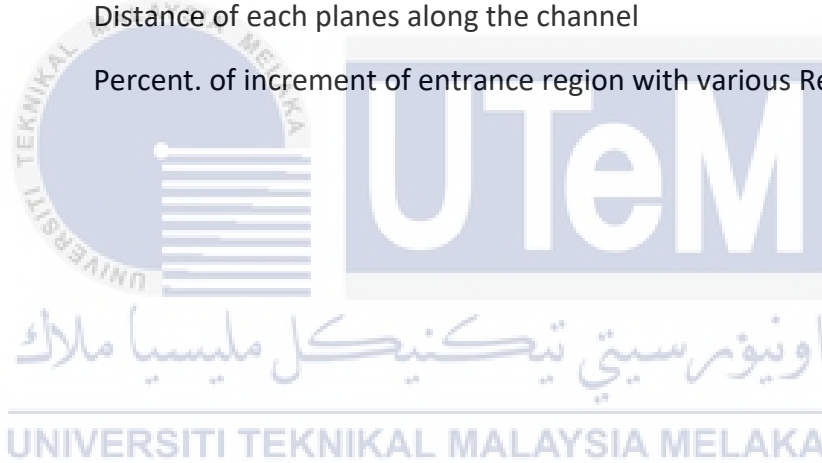


LIST OF FIGURES

Figure	Title	Page
1.0	Fluid flow varies along contact geometry	13
3.1	General methodology done in present study	27
3.2	Schematic of rectangular microchannel unit cell	28
3.3	Meshed domain viewed from top	29
3.4	Meshed domain viewed form the inlet	29
3.5	Dimension of unit cell of microchannel	30
3.6	Properties of nanofluid	33
4.1	Nusselt number to different meshed sizes	35
4.2	Mesh independence test for different meshed sizes	36
4.3	Comparison of average Nusselt number at Re=140	37
4.4	Cross-sectional planes of fluid flows	39
4.5	Fluid velocity at the middle plane of fluid channel	41
4.6a	Velocity profiles of fluid flows at Re=140	41
4.6b	Velocity profiles of fluid flows at Re=300	42
4.6c	Velocity profiles of fluid flows at Re=500	42
4.7	Velocity profiles at Plane 1, 2, 3 and 4	43
4.8	Temperature distribution in x – y plane	44
4.9a	Middle plane heat sink (z=0.05mm)	45
4.9b	Side plane heat sink (z=0.0125mm)	45
4.10	Reynolds number on top wall of fluid channel	47
4.11a	Heat flux of Re =140 at channel fluid contact region	48
4.11b	Heat flux of Re =300 at channel fluid contact region	48
4.11c	Heat flux of Re =500 at channel fluid contact region	49
4.12	Comparison of average Nusselt number	51

LIST OF TABLES

Table	Title	Page
2.1	Result of critical Re determined by previous researchers	24
3.1	Boundary-type specifications for domain	31
3.2	Continuum type of specifications	31
4.1	Distance of each planes along the channel	39
5.1	Percent. of increment of entrance region with various Re	51



LIST OF ABBREVIATIONS

CFD	Computer Fluid Dynamic
SIMPLE	Semi- Implicit Method for Pressure Linked Equations



LIST OF SYMBOL

A_c	=	Area of cross section, m^2
a	=	Width of the entrance of fluid channel, m
b	=	Height of the entrance of fluid channel, m
D_h	=	Hydraulic diameter, μm ($D_h=4A/P$)
P	=	Perimeter of entrance of fluid channel, m
k	=	Thermal conductivity, W/m.K
L_{ch}	=	Length of the channel, m
H_t	=	Height of a single reentrant cavity, m
N	=	Number of channel
Nu	=	Nusselt number
Pa	=	Static pressure, Pa
q''	=	Heat flux, W/cm^2
Re	=	Reynolds number
T	=	Temperature, K
u	=	Fluid velocity, m/s

SUBSCRIPT

nf	=	Nanofluid
Al_2O_3	=	Aluminium Oxide/Alumina
Avg	=	Average

CHAPTER 1

Introduction

1.1 Background of Study

Fluid flow in micro-passages such microchannel in current studies have developed to meet the demand for thermal-hydraulic control of microsystem. The research on microsystem analysis has developed from time to time in achieving low thermal resistance in micro-electronics industry.

Fluid flow in general can be characterized to three different stages which are laminar, transition and turbulent. The movement of adjacent fluid particles in highly ordered motion and smooth streamlines shows the fluid are in laminar motion whereas turbulent can be characterized by velocity fluctuations and highly disordered motion of fluid flow. The transition from laminar to turbulent flow is unsteady and difficult to predict, it happens over some region where fluid flow fluctuates between laminar and turbulent before it becomes fully develop region (Cengel & Cimbala, 2014).

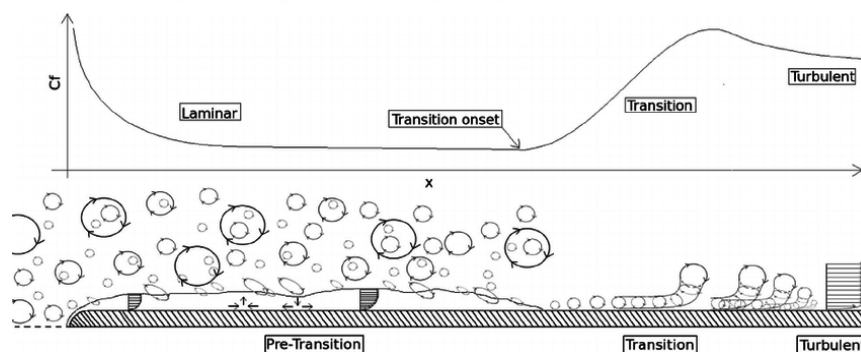


Figure 1.0 Fluid flow varies along contact geometry (Coronella, 2008)

Osborne discovered that flow regime depends mainly on the ratio of inertial forces to viscous forces in the fluid. This ratio is called Reynolds number and when the fluid becomes

turbulent, the Reynolds number at that point is called critical Reynolds number (Osborne & Incropera, 1985).

It is better to have an accurate values of Reynolds number in determining the flow region of liquid flows as studied made by (Cengel & Cimbala, 2014) in macro-scale study. For macroscale study, the Reynolds number in transition from laminar to turbulent flow under most practical conditions is in the range of $0 \leq Re \leq 4000$ for liquid flow inside macrochannel. That is,

$$Re \leq 2000, \text{ laminar flow}$$

$$2000 \leq Re \leq 4000, \text{ transitional flow}$$

$$Re \geq 4000, \text{ turbulent flow}$$

The critical Reynolds number at which the flow become turbulent is different for different geometries and flow conditions. Avoiding flow disturbances and pipe vibrations in such carefully controlled laboratory experiments could maintain the Reynolds numbers.

Microchannels are defined as flow passages that have hydraulic diameters in the range of 10 to 200 micrometers. The evolution of microchannel have developed to several decades of improvements and received considerable attention in major application areas, such as advanced heat sink designs and micro fuel cell system. The development of understanding the fluid flow in microchannel is essential for the optimum design and effective operation of the microsystem. In this study also, the flow of the fluid inside the microchannel is analysed numerically with dimension of the microchannel for the fluid flows are $57 \mu\text{m} \times 180 \mu\text{m}$ with length of 10mm. Two solid boundaries are separated with walls and fluid flows of the microchannel.

The working fluid used in the study is Alumina nanofluid, Al_2O_3 and water with volume fraction of 1% and 1-100nm nanoparticles. Alumina nanofluid, Al_2O_3 is chosen due to its properties of good convection heat transfer for micro-cooling technologies and any other micro-scale channels.

1.2 Problem Statement

Reynolds number is very significant in nanofluid microchannel flows to determine the flow and heat analysis throughout the micro-scale system. However, the applicability of Reynolds number in micro-scale system is still under investigation whether it is usable for micro-scale system or not. Hence, this study is done to investigate the Reynolds number in nanofluid-microchannel flow together with the applicable of this Reynolds number range for macro-scale channel to the micro-scale channel.

1.3 Objectives

There are two main objectives in this study which are:

1. To simulate the nanofluid flow at various Reynolds number.
2. To investigate the velocity profile of nanofluid flow at various Reynolds number.

1.4 Scope of Project

The scopes of this project are:

1. The microchannel is rectangular in shaped with hydraulic diameters maximized to $200\mu m$.
2. Reynolds number of 140 – 500 are investigated in the studies.
3. Alumina nanofluid, Al_2O_3 with kinematic viscosity of $0.001028 \text{ kg/ms}^{-1}$ and concentration of 1% as the working fluid used in the study.
4. The heat flux of 90 W/cm^2 is constant throughout the channel as the heater is located at the top wall of the fluid channel.

1.5 General Methodology

As to achieve good computational fluid dynamics results, the steps below are to be followed accordingly.

1. Literature review

Journals, articles, or any materials regarding the project will be reviewed.

2. Pre-processing (Designing)

Fluid flows in turbulent and the fluctuation of critical Reynolds number will be defined and determined through the analysis of research. The velocity profile of nanofluid flow at various Reynolds number will be identified through designing of the microchannel at the operating condition.

3. Solver (Mesh Generation)

The design of the microsystem is decomposed into cells with structured quadrilateral geometry specified to the design proposed. This discretization process acquires good meshing size with correct estimation of spatial derivatives to obtain good meshing result.

4. Post-processing (Numerical)

Velocity profile of nanofluid flows is analysed through Fluent 6.1 with generated meshed volume of microchannel.

5. Validation

The numerical result must be tallied to the proposed data to achieve a correct fluid velocity profile at various Reynolds number (Esionwu-k, Marker, & Claus, 2014).

CHAPTER 2

Literature Review

2.1 Introduction

This literature review will be focussing on the nanofluid flows inside microchannel. The objectives of this study are to identify velocity profile and to simulate nanofluid flow inside microchannel. In this chapter, previous studies that are related to nanofluid flows in microchannel are reviewed. The findings of this studies are studied and summarized in the form of tables and figures. This chapter is separated into three parts which are nanofluid characteristics, significance of nanofluids in relation to Reynolds number and factors affecting the nanofluid flows.

2.2 Nanofluid Characteristics

Several scholars have taken numerous studies about the nanofluid over centuries. At present, water and refrigerants are commonly used as working fluids inside microchannel, the mixture of conventional fluids is proposed with the use of nanoparticles (1-100 nm in diameter) to improve the heat transfer performance of conventional fluids by enhancing thermal conductivity inside the microchannel. The use of nanofluids have proved to be a very effective way for cooling systems inside microchannel due to nanoparticle separation to the base fluid. It has been proved that nanofluids have better heat transfer performance than the base liquid and a good substitutional for working fluids inside microchannel (H. Zhang, Shao, Xu, & Tian, 2013).

Recently, the study of different nanofluid such as CuO-water or Al_2O_3 -water has been a great interest among researcher in improving thermal performance of nanofluids flow in microchannel. (Jung, Oh, & Kwak, 2009) examined the performance of alumina (Al_2O_3) with a diameter of 120 nm nanofluids with various particle volume fractions shown an increment of

32% rather than distilled water at a volume fraction of 1.8% volume percent without major friction loss.

The study of nanofluid flow characteristics of low Reynolds number around a heated circular cylinder are studied by (Vegad, Satadia, Pradip, Chirag, & Bhargav, 2014) which resulted to increment of local Nusselt number over cylinder surface in nanoparticle fraction as well as increment of nanofluids flow strength. The study proved that local heat flux drops along cylinder wall while nanoparticles fraction increased together with Reynolds number along the cylinder wall until the outlet.

2.3 Reynolds number and its significance.

There are many experimental researches that have been done by researchers in configuring fluid flow and thermal conductivity inside microchannel. Experiments on flow characteristic at very low Reynolds numbers for liquid flow in microchannel have been done by Xiwen Zhang (X. Zhang et al., 2016). They tested deionized water and kerosene in rectangle cross-section microchannel with width $2.7 - 20 \mu\text{m}$ and depth of $20 - 45 \mu\text{m}$ under very low Reynolds number condition ($10^{-5} \leq \text{Re} \leq 10^{-2}$) thus provide a correlation to the flow of Newtonian fluid in a smooth micrometer-sized consistent with classical theory of laminar flow.

Experiment on effect of the inlet conditions in the transition region has been performed by (D.V., J., & J.P., 2014) with three different inlet geometries of 1.05 mm, 0.85 mm, and 0.57 mm with equal length of 200 mm. The use of water as cooling fluid inside single copper microchannel are tested which resulted to the enhancement of friction factors and Nusselt numbers for critical Reynolds number of 2000. (Kim, 2016) Byongjoo Kim has performed a study to explore the validity of theoretical correlations in predicting fluid flow and heat transfer characteristics based on conventional sized of microchannel. 10 different rectangular microchannels with hydraulic diameter of $155 - 580 \mu\text{m}$ and Reynolds number ranging from 30 to 2500 are tested. The critical Reynolds number of 1700 to 2400 are obtained with decreased of aspect ratio from 1.0 to 0.25. The single phase laminar friction factors in the microchannel has obeyed to the conventional Poiseuille flow theory.

Investigation of three dimensional heat transfer in silicon microchannel by (Qu & Mudawar, 2002) proved that the temperature rise along the flow direction in the solid and fluid can be approximated as linear. The length of the flows developing region are affected by increasing Reynolds number to 1400 which fully developed flow may not be achieved as Reynolds number are affected by the thermal conductivity as it approaching to the channel outlet. Measured temperature distribution is well predicted by CFD prediction on validity of conventional theory and numerical solution of laminar Navier-Stokes equations as correlations used in comparisons.

2.4 Factors affecting fluid flow of nanofluid

(Peiyi & Little, 1983) has reported that there are many factors in which affecting the fluid flow and at the same time affecting the value of the friction factor in microchannel. Surface roughness is one of the factors that affects the fluid flow from transition to turbulent mostly by increasing of drag coefficients in turbulent flow in microscale channel. In this case, significant roughness is presented but friction factors measured in smooth channel agreed with macroscale theory -in rectangular microchannel. Thus, making the friction factor too small that it can be negligible in this microchannel.

There are two parameters that essential to Reynolds number in nanofluid studies whereas there are the inlet velocity and the kinematic viscosity of nanofluid which the Reynolds number are depended on. To keep the Reynolds number constant for heat transfer enhancement in the microchannel, the increment of inlet velocity has a major role in reaching constant Reynolds same as important of increment of nanoparticles volume fraction of nanofluid (Akbarinia, Abdolzadeh, & Laur, 2011).

The flow instabilities, uncommon heat transfer rates and increased pressure drop caused by fluid acceleration during phase change persist as important look out on the experimental investigation on the microchannel. Stability of nanofluid to application areas of nanofluid are studied by (ŞİMŞEK, 2016) together with the effect of surfactant, lowering the surface tension on the thermal performance and pumping power of nanofluids in microchannel. The comparison of convection heat transfer coefficient and pumping power for different coolant are performed in achieving a steady laminar flow in the micro scale channel. The experiments are

performed using spherical gold nanoparticles of (10, 50 and 100 nm), volumetric concentration of (0.00064% - 0.0052%) and flow rate of (100 – 140 $\mu\text{m}/\text{min}$) on the nanofluid performance of 70 μm x 50 μm rectangular copper microchannels in determining the surfactant effect.

Considering particle migration of nanofluid, particle clustering and particle interactions with the wall, the nanofluid flow are affected due to possible heat transfer enhancement with more complex nanoparticle-based fluid interactions as well as different preparation methods in preparing nanofluid that lead to inconsistencies in research projects on nanofluids. The study of particle migration on nanofluid is performed (Bahiraei, 2016) by taking Brownian motion and viscosity of nanofluids into account in stabilizing nanoparticle along the microchannel.

In addition, in this paper the study of heat transfer are discussed thoroughly together with thermal conductivity, heat dissipation and convective heat transfer inside fluid channel as it is counter related to the objectives of the study in identifying velocity profile and simulate nanofluid flow inside microchannel.



Table 2.1 Result of critical Re determined by previous researchers.

Author	Nanofluid	Hydraulic Diameter	Results	Remarks
Tuckerman & Pease (1981)	Water	86 μm - 95 μm	Critical Re = 2300	constant heat flux
Dirker et al. (2012)	Water	$h_d = 1.05, 0.85, 0.57$ mm. length = 200 mm,	$1800 \leq Re \leq 2300$, Cr Re = 2000	Enhancement of friction factors and Nusselt number due to the effect of the inlet condition
Trinh (2016)	Deionized water and FC770	10 mm	Re = 30 - 2500	To explore the validity of current studies
Weilin Qu, Issam Mudawar (2002)	Water	width = 57 μm , depth = 180 μm , distance wall = 43 μm	Critical Re = 1400	Navier-Stokes equation as comparison used as correlations
Byongjoo Kim (2016)	Water	Aspect ratio = 1.0 - 2.5	Re = 1700 - 2400	Validity of theoretical correlations based on conventional sized channels
Jung, Hoo and Kwak. (2009)	Aluminium dioxide, Al ₂ O ₃	170 nm	Re correlated to thermal conductivity of nanofluids.	Investigate the effect of volume fraction of nanoparticles to convective heat transfer and fluid flow in microchannel
Choi et al. (2002)	Water	53 μm and 81.2 μm 9.7 μm and 6.9 μm	Critical Re= 2000 Critical Re= 500	Thermal conductivity increased with increase of grain size

Wu and Little (1983)	Water	45.5 μm and 83.1 μm	$\text{Re} < 1000$ = laminar $\text{Re} > 3000$ = turbulent 900-3000 = transition	Glass and silicon channels
Hegab et al. (2002)	R134a	112 μm to 210 μm	Transition = 2000 to 4000	Aluminium Microchannel
Yu et al. (2014)	Methanol	57 μm - 267 μm	$\text{Re} = 50$ -850	Early laminar transition does not exist.
Zhang et al. (2013)	Nanofluids Al2O3	5.0 μm - 17.4 μm	$\text{Re} = 600$ - 20000	$\text{Pr} = 5.7$ - 7.3, nusselt correlation to Pr number.
Judy et al. (2002)	Water	50 μm - 100 μm	Critical $\text{Re} = 2300$	Adiabatic boundary condition for silica microchannel and single-phase flow
	Methanol	15 μm - 150 μm		
	Isopropanol	75 μm - 125 μm		

CHAPTER 3

Methodology

3.1 Introduction

This chapter provides a detail description of the methodology or how this whole project proceeds. This chapter also focus on what kind of method being used to obtain the necessary data for velocity profile and nanofluid flow inside microchannel. As can be observe in the flow chart provided in Figure 3.1, the figure shows the step required to successfully achieve the aim of the study in finding critical Reynolds number of nanofluid in transition flows inside microchannel.

The microchannel is created in 3D domain using GAMBIT software. After successfully created the volume of 3D domain, the 3D domain is meshed throughout each surfaces of the volume by aligning the node number to correct estimation. This cells with structured quadrilateral geometry need to be designed closely to one another at the inlet and getting distant as it come out to the outlet which results to velocity profile and critical Reynolds of nanofluid in the microchannel.

When the design and meshing process are done, the domain is analyzed through FLUENT ANSYS 6.1 computer software whereas the simulation data is obtained in relation to the analytical solutions on available resources.

The methodology of this project is summarized in the flow chart as shown in Figure 3.1.

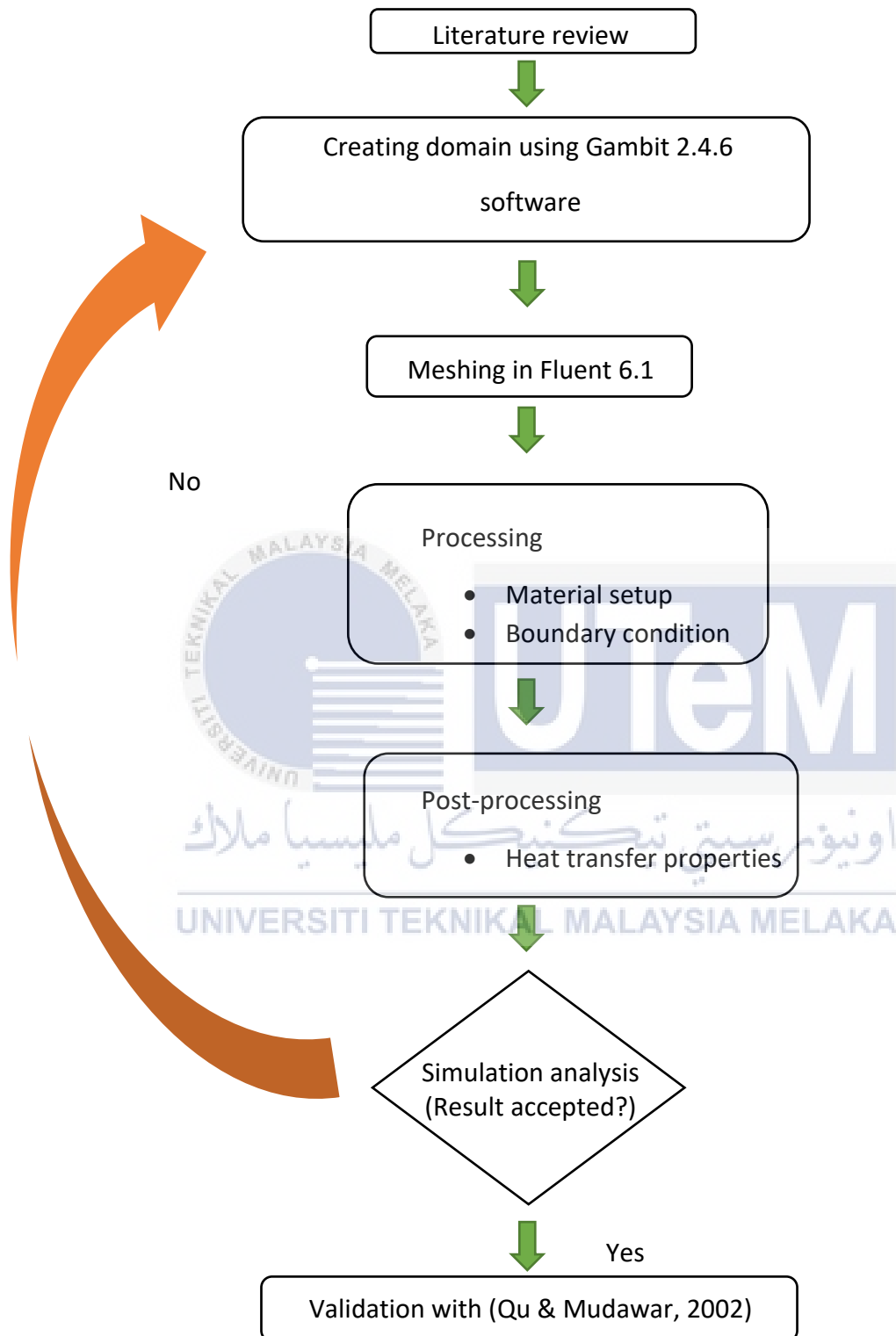


Figure 3.1 General methodology done in research

3.2 3D Design Domain

The rectangular microchannel is designed using Gambit software to obtain the analytical result of nanofluid flow. This process is essential as it will determine the fluid characteristics and velocity profile at the end of the experimental investigation. Design process is done using Gambit software with specifications as in Figure 3.2 with respect to thermal conditions of silicon rectangular microchannel. All the dimensions of the microchannel are same as previous work done by (Qu & Mudawar, 2002).

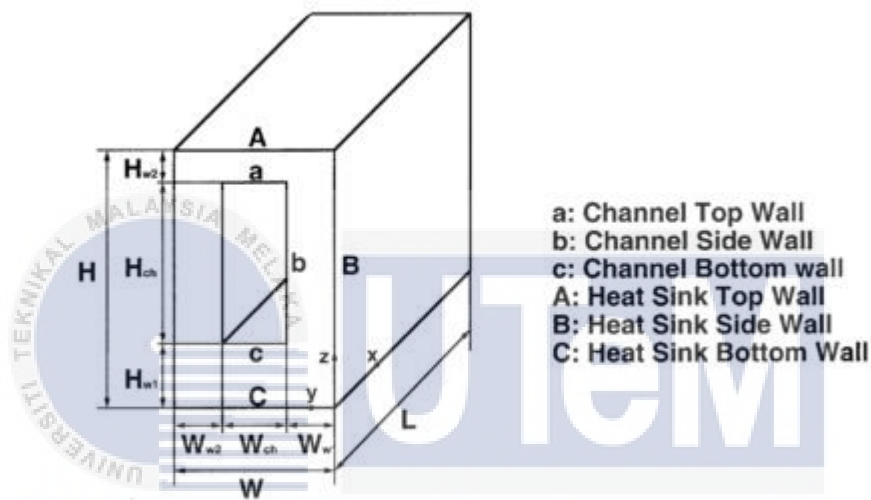


Figure 3.2 Schematic of rectangular microchannel unit cell (Mudawar, 2002)

3.3 3D Modelling Mesh Discretization

Domain is meshed using structured quadrilateral cells on each surface of the microchannel. The node number of every surfaces are determined with perfect balance from the inlet to the outlet of the rectangular microchannel. Whereas the range of the cells should be in closely manner to one another on the inlet and lengthen towards the outlet. This specific action is taken in a way to achieve good computational fluid dynamics result of the nanofluid flow together with an ideal velocity profile from laminar to turbulent inside the microchannel.

Moreover, the 3D modelling meshed volume of rectangular microchannel is exported into computer simulation software of Ansys Fleunt 6.1 in determining fluid velocity with heated surface on the topwall and enclosed with solid wall. The microchannel is analyzed with

nanofluid as the cooling fluid with a width of 57 μm and depth of 180 μm . The result is validated by comparing the predictions with analytical solutions and available experimental data.

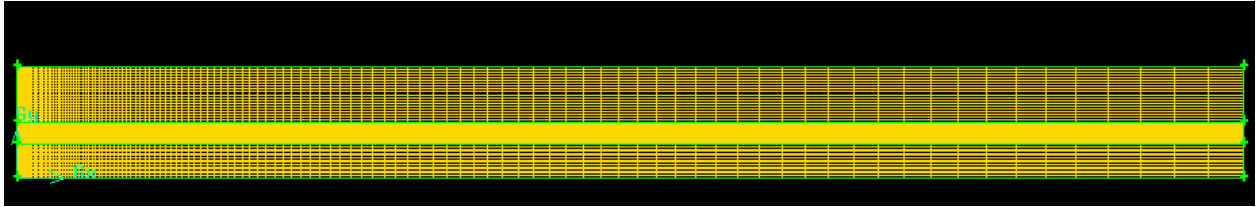


Figure 3.3 Meshed Domain viewed from top

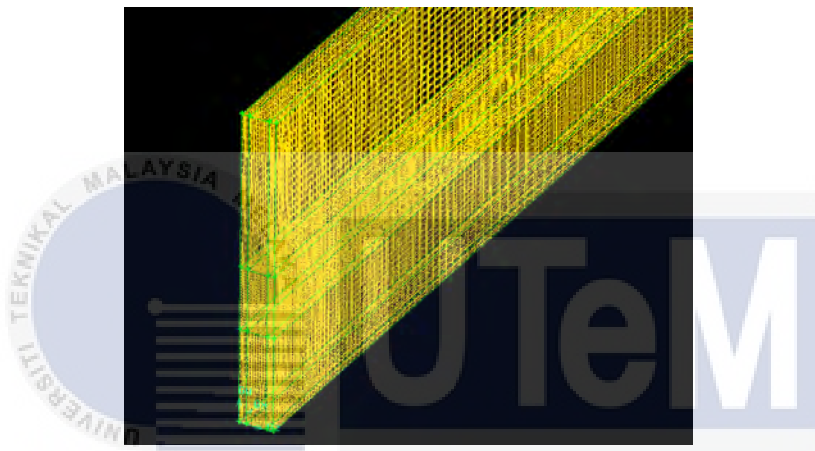


Figure 3.4 Meshed Domain viewed from the inlet

Table 3.5 shows the dimension of the microchannel as in Figure 3.2. All the dimensions of the microchannel are same as previous work done by (Qu & Mudawar, 2002).

Figure 3.5 Dimension of unit cell of microchannel

W_{w1} (μm)	W_{ch} (μm)	W_{w2} (μm)	H_{w1} (μm)	H_{ch} (μm)	H_{w2} (μm)	L (mm)
21.5	57	21.5	270	180	450	10

This meshed volume is form in hexagonal quadrilateral for every surface where it covered whole volume of microchannel for every node. The analysis continued as the fluid flows inside the microchannel, the nanofluid flow pattern is studied in laminar motion of nanofluid particles with several Reynolds before it become turbulent. The hexagonal quadrilateral meshed volume resolved the velocity profile of the fluid flow towards increasing of fluids movement as it goes towards the outlet.

3.4 Boundary Conditions

Boundary condition of the model are defined with physical and operational characteristics of the model at its boundaries and within specific regions of its domain. There are two zone-type specifications in creating the boundary conditions of the model which are boundary types and continuum types. Boundary-type specifications defined the characteristics of the model at its external or internal boundaries and continuum-type specifications defined characteristics of the model within specified regions of its domain. Boundary-type specifications for the domain are simplified in Table 3.1 while the continuum-type specifications are in Table 3.2.

Table 3.1 Boundary-type specifications for domain

Entity	Zone type
Face 1	Velocity Inlet
Face 2	Pressure Outlet
Face 3	Heater

Table 3.2 Continuum type specifications

Entity	Zone type
Face 4	Solid
Face 5	Fluid

The boundary conditions are figured with conventional theory of Navier-Stokes equation as correlations in studies. Some main assumptions are required for conventional Navier-Stokes and energy equations to model the heat transfer process whereas:

- 1- Laminar flow
- 2- Steady fluid and heat transfer
- 3- Incompressible fluid
- 4- Constant solid and fluid properties
- 5- Negligible radiation heat transfer
- 6- Negligible superimposed natural convective heat transfer

The whole unit cells are chosen as the unitary domain in this investigation. For the hydraulic boundary conditions, the velocity is equal to zero for all boundaries except the channel's inlet and outlet. A uniform velocity is applied at the channel inlet.

$$u = \frac{Re \cdot \mu_f}{d_h}, v = 0, w = 0$$

for $x = 0, W_{w1} \leq y \leq W_{w1} + W_{ch}$, and $H_{w1} \leq z \leq H_{w1} + H_{ch}$

The flow at the channel outlet is assumed to be fully developed.

$$\frac{\partial u}{\partial x} = 0, \frac{\partial v}{\partial x} = 0, \frac{\partial z}{\partial x} = 0,$$

for $x = L, W_{w1} \leq y \leq W_{w1} + W_{ch}$, and $H_{w1} \leq z \leq H_{w1} + H_{ch}$

For the thermal boundary conditions, all walls of the solid region are treated as adiabatic boundary condition except the base wall of the heat sink, where a constant heat flux is assumed.

$$-k_s \frac{\partial T}{\partial z} = q^n, \text{ for } 0 \leq x \leq L, 0 \leq y \leq W, \text{ and } z = H$$

At the channel inlet, a constant inlet temperature is applied.

$$T = T_{in}, \text{ for } x = 0, W_{w1} \leq y \leq W_{w1} + W_{ch}, \text{ and } H_{w1} \leq z \leq H_{w1} + H_{ch}$$

The flow is fully developed when it approaches the channel outlet,

$$\frac{\partial^2 T}{\partial x^2} = 0, \text{ for } x = L, W_{w1} \leq y \leq W_{w1} + W_{ch}, \text{ and } H_{w1} \leq z \leq H_{w1} + H_{ch}$$

At the fluid-solid interface, no-slip and no-penetration wall condition is assigned.

$$u_i = 0$$

Coupled wall boundary conditions are also applied on the solid-fluid interface to couple up the fluid convection and solid conduction.

$$T_s = T_f - \lambda_s \left(\frac{\delta T_s}{\delta n} \right) = \lambda_s \left(\frac{\delta T_f}{\delta n} \right)$$

3.5 Thermal properties

The thermal properties of the nanofluid is stated in Figure 3.6.

Properties	
Density (kg/m³)	constant 1027.92
Cp (J/kg-K)	constant 4050.03
Thermal Conductivity (W/m-K)	constant 0.631
Viscosity (kg/m-s)	constant 0.001028

Figure 3.6 Properties of nanofluid

CHAPTER 4

Results

4.1 Introduction

In this section, the validation of the simulation is done, and the result of the simulation will be shown and discussed. The velocity profile and wall shear stress along the x-direction of the microchannel are plotted on the chart. The Nusselt number along the channel is obtained to plot a graph and shown the effect of the design on cooling effects.

4.2 Mesh Independence Test

To find out the best meshing sizes with the lowest nodes for the geometry design, a grid independence test is carried out which intended to reduce the simulation time and reduces the iteration to reach convergences as low as possible. A few different meshing with various amounts of nodes are created and simulated.

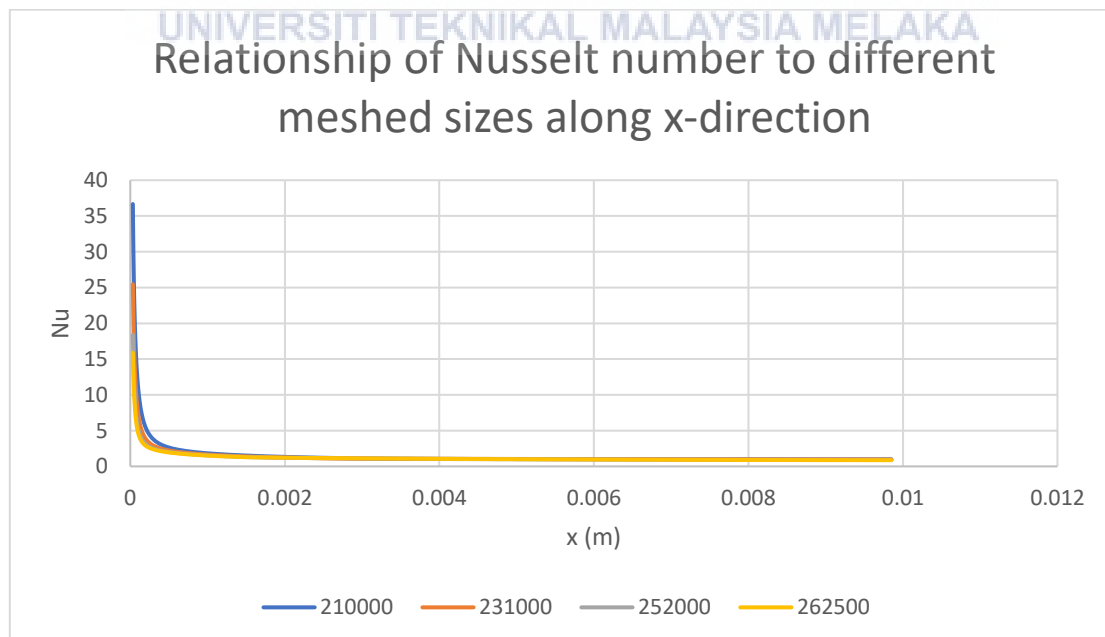


Figure 4.1 Relationship of Nusselt number to different meshed sizes along x-direction

As shown in Figure 4.1, the grid dependence test is conducted by using several different numbers of cells at the z plane of the channel inlet. Nanofluid flows with velocity of 5.78 m/s is used in determining the best-fit Nusselt number in fully develop region. To find out the best meshing size for the nanofluid flows in the microchannel, results on Nusselt number at fully develop region at 0.002 m is plotted in Figure 4.2.

The average peripheral Nusselt number at the outlet of the for different mesh sizes are calculated and plotted at Figure 4.2. The meshing is considered as grid independence if the average Nusselt number remain constant even though the number of nodes is increasing.

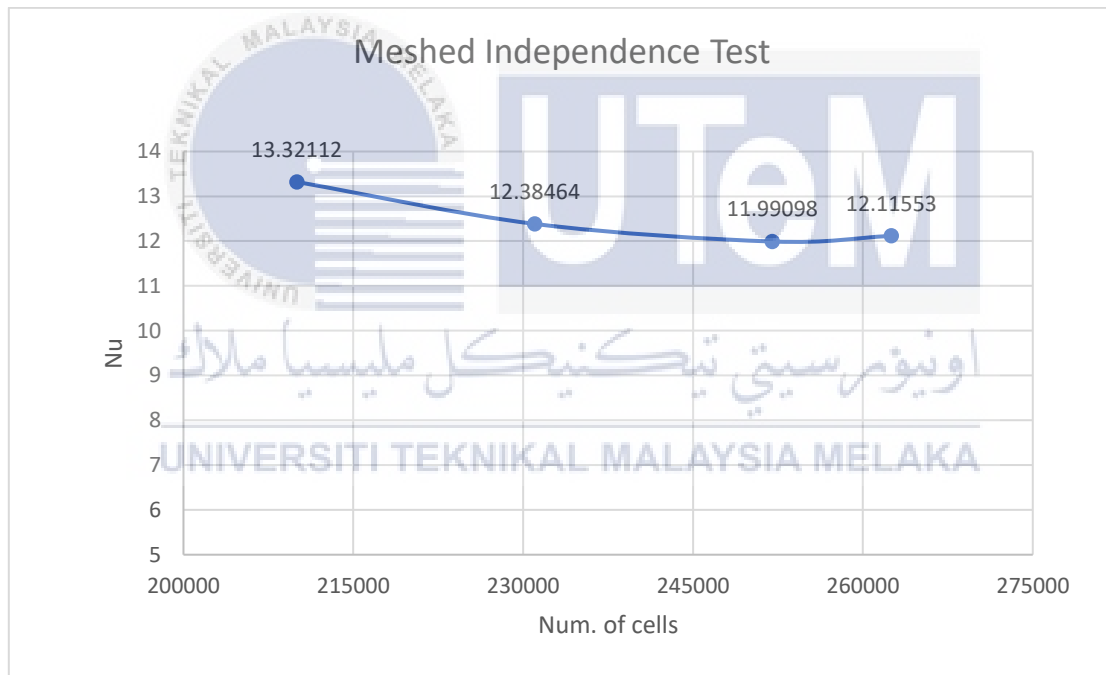


Figure 4.2 Meshed independence test for different meshed size

As shown in Figure 4.2, the average Nusselt number remains constant at 12 from 250 thousand number of cells and onwards. The correlation of number of cells to the constant value of Nusselt number indicated that meshing sizes with 250 thousand number of cells will reach the convergences and reduce the iterating time sooner and at the same time proved that the meshing sizes are equally distributed along the channel.

4.3 Validation

To ensure the simulation analysis of the nanofluid flows is valid, the numerical code is verified by comparing it with available analytical solution or widely accepted numerical results.

The surrounding solid boundary is removed, and a pure convective heat transfer characteristic is considered. The energy equation was verified. Constant longitudinal heat flux with uniform peripheral heat flux is set as the boundary condition. The Reynold's number is set to 140 for validation purposes. From the simulation result, the peripheral Nusselt number, Nu is calculated and plotted in Figure 4.1 against the length of the microchannel, L .

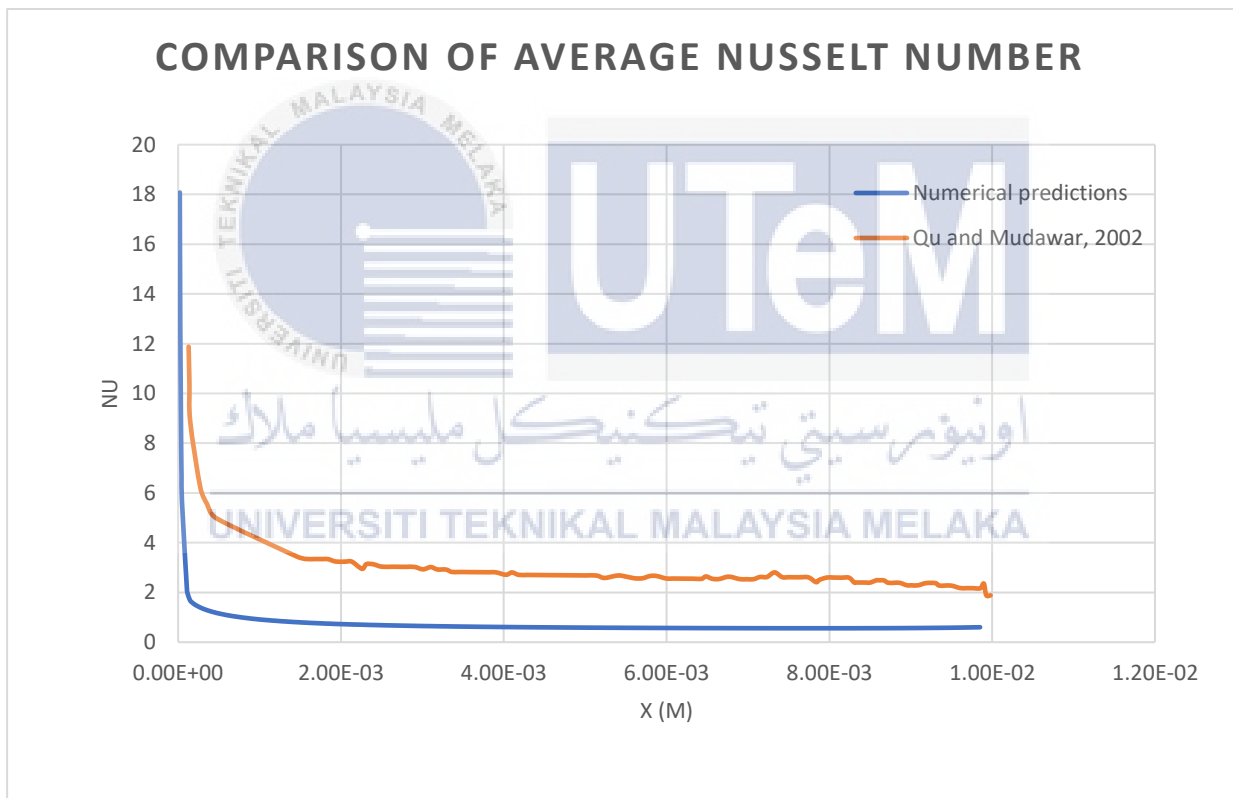


Figure 4.3 Comparison of average Nusselt number at $Re = 140$.

Nu is calculated using formula below.

$$\text{Nu} = \frac{q'' D_h}{K_T(T_{T,m} - T_m)}$$

Where $T_{T,m}$ is the average temperature at the contact surface

$$T_{T,m} = \frac{1}{T} \int_T T_T dT$$

T_m is the fluid bulk temperature

$$T_m = \frac{\int_T uT dA_c}{\int_T u dA_c}$$

The calculated result of Nusselt number is used to compare the present straight microchannel results of (Qu & Mudawar, 2002), which is plotted in Figure 4.3. The calculated result which shown similarities to the previous work, where the Nu at the channel inlet is high and drop rapidly and approaches constant value at fully developed region to the outlet. The largest deviation between simulation result and Qu's result is approximately 8.8%. Therefore, the simulation is considered as valid since the simulation is showing an identical result pattern as Qu and Mudawar works. Other design which have the same setup of microchannel proves that the simulation for other designs are acceptable too.

4.4 Velocity Profile

In simulating the fluid flow inside the microchannel, a straight line at few planes of cross sectioned of the fluid channel in Y-axis are created as in Figure 4.4. The distances of the cross sectioned lines are taken at starting region and at the developed region of the fluid flows in a microchannel. This action is taken to provide a straight velocity profile for the fluid flows in longitudinal x – axis from inlet to the outlet.

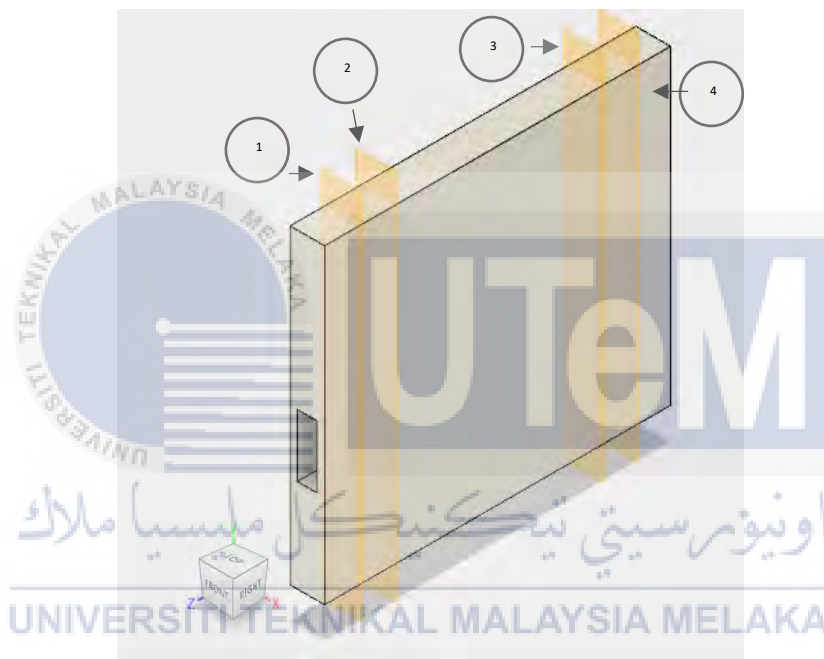


Figure 4.4 Cross-sectional planes of fluid flows.

Table 4.1 The distances of each of the planes along the channel.

Number of planes.	1	2	3	4
Distance (m)	0.001	0.0018	0.008	0.009

Based on fluid velocity shown in Figure 4.5, the results concluded that the developing region or entrance length are increasing as the Reynolds increased. Reynolds number of 140 has too small entry length approximately at 0.5 mm, about 2.36% of velocity increment with respect to entry length while Reynolds number of 300 has 2 mm entry length with 4.47% velocity increment. These numbers are increasing as Reynolds increased, the percentage of velocity increment increased up to 11.63% before it reached fully developed region at 4.0 mm.

The results of each velocity profiles are illustrated in Figure 4.6a, b and c where it shown that the velocity of nanofluid increasing linearly as it moved towards the outlet. Low Reynolds number has relatively small starting region approximately less than 4 mm and the difference became more pronounced at high Reynolds number as indicated at Figure 4.5. Increasing of Reynolds number shown that the velocity magnitude also is increasing as it moves towards the outlet thus making the velocity profiles more apparent.

Based on Figure 4.6a, fluid inlet velocity of 1.62m/s is increasing towards Plane 1 at 2.88m/s and continued towards Plane 2 with fluid velocity 2.90m/s which are still in underdeveloped region. Condition where the fluid is still in starting region with very low Reynolds number made the entrance effects is negligible. However, the fluid velocity became constant at developing region; Plane 3 and 4, with velocity magnitude of 2.94m/s until it reaches the outlet of the microchannel.

Moreover, the parabolic velocity profiles with Reynolds number of 300 and 3.47m/s fluid inlet velocity in Figure 4.6b also increases toward plane 1 at 6.0m/s and continued towards Plane 2 of velocity 6.3m/s. Alike to Reynolds number of 500 with fluid inlet velocity of 5.78m/s at Figure 4.6c, the velocity increases to 9.8m/s at Plane 1 and continued towards plane 2 of velocity 10.3m/s.

The parabolic velocity profiles become more pronounced as the fluid velocity magnitude become constant in flow direction through Plane 3 and 4 with velocity of 6.5m/s for $Re=300$ and 10.6m/s for $Re=500$, in which the flows are in fully developed region and the velocity profiles are essentially identical.

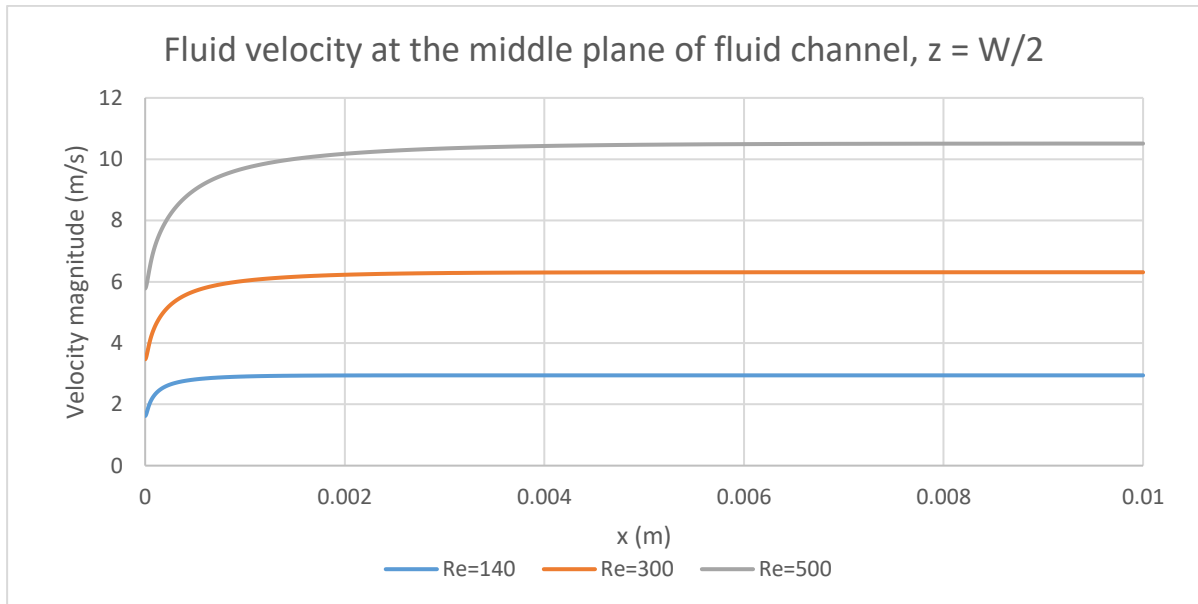


Figure 4.5 Fluid velocity at the middle plane of fluid channel.

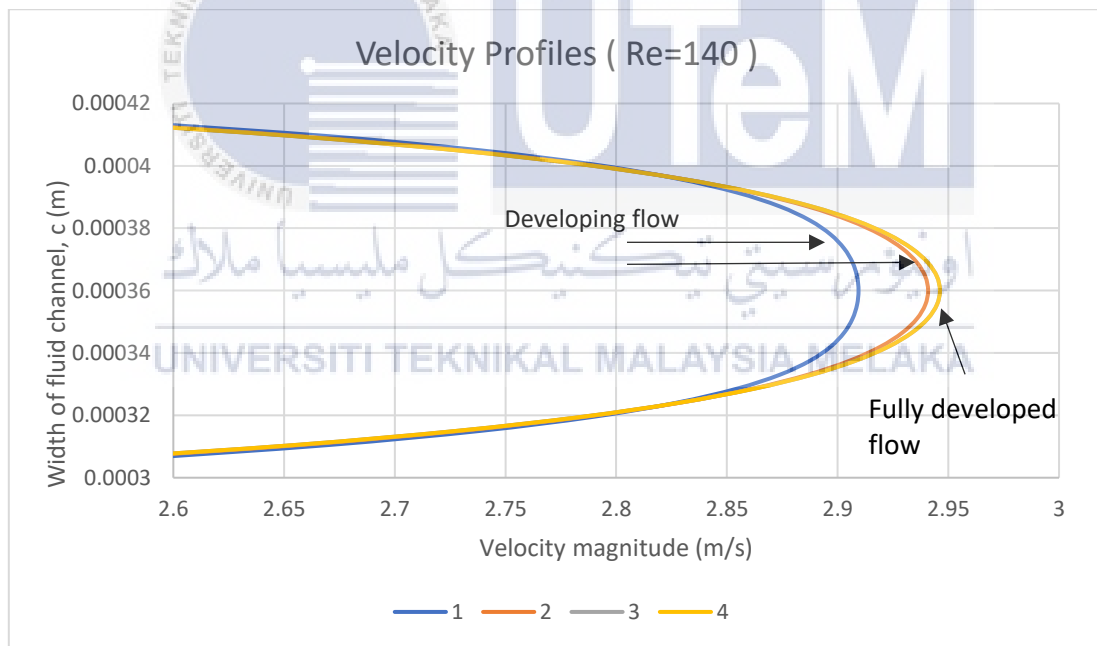


Figure 4.6a) Velocity profiles of fluid flows at Re=140

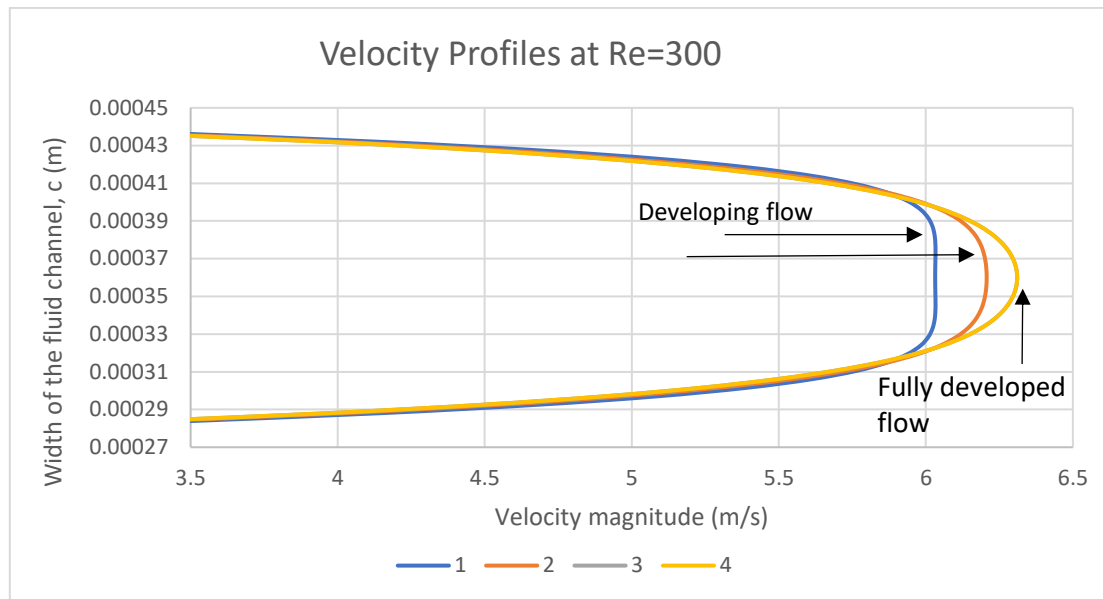


Figure 4.6b) Velocity profiles of fluid flows at $Re=300$

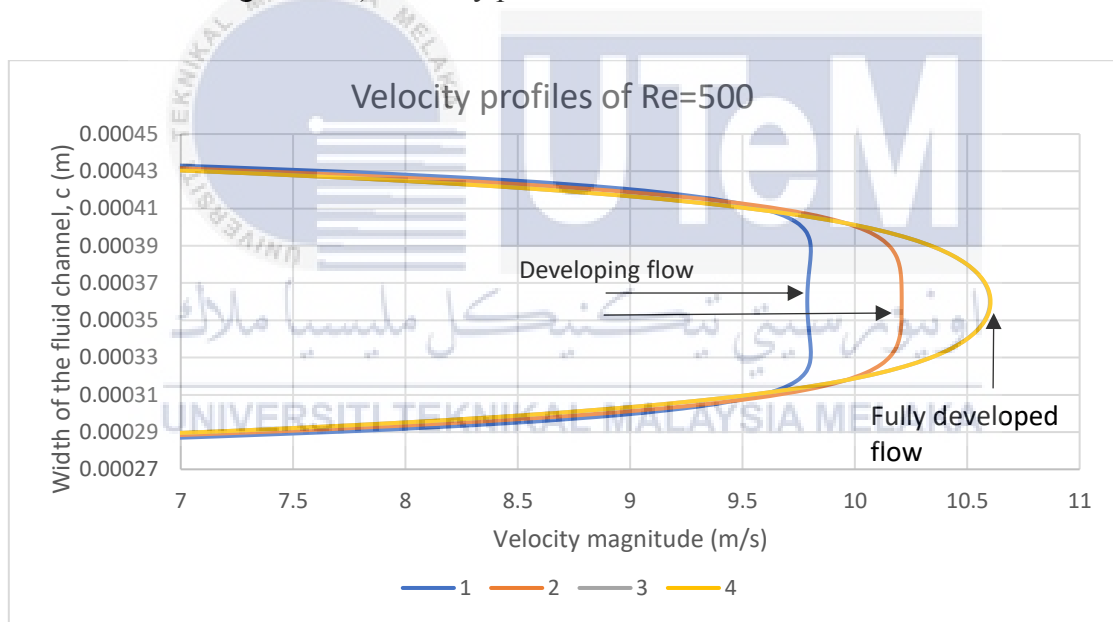


Figure 4.6c) Velocity profiles of fluid flows at $Re=500$

The correlation of planes located in $y - z$ direction towards its longitudinal x -axis is required in achieving straight velocity profiles throughout the microchannel, thus making Plane 1 and Plane 2; underdeveloped region, and Plane 3 and Plane 4 in fully developed region. Velocity profiles as shown in Plane 3 and Plane 4 in which the flows are in fully developed, are constant and identical for Reynolds of 140, 300 and 500 as shown in Figure 4.6a, b and c, respectively. The constant velocity profiles results to constant laminar flow throughout the microchannel with no critical Reynolds achieved. Low Reynolds numbers used resulted to low entrance region at each Re , where the entrance effect is negligible.

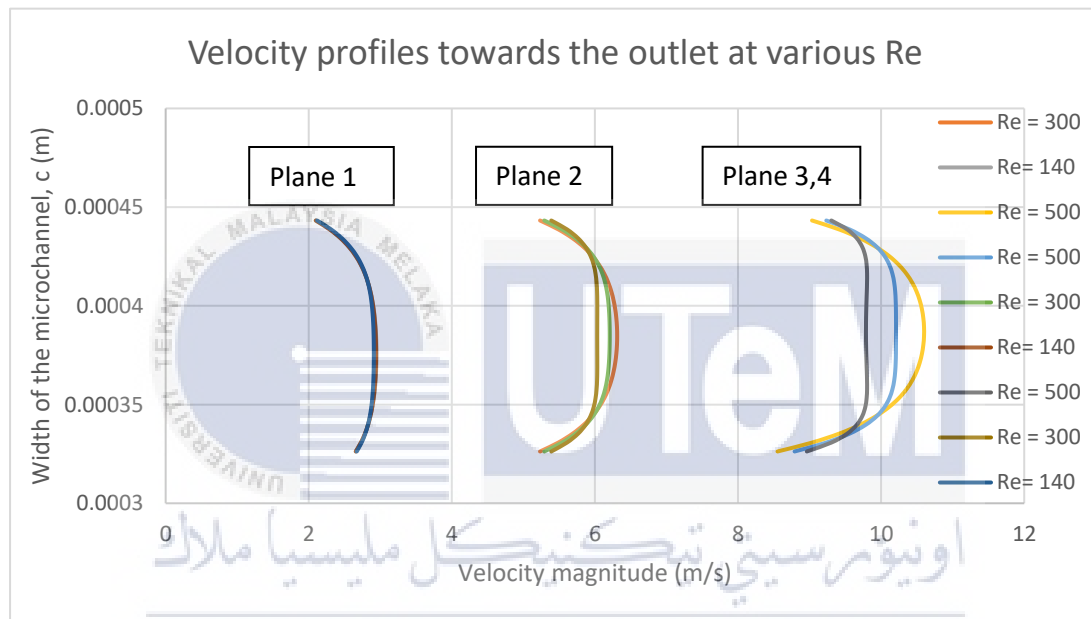


Figure 4.7 Velocity profiles towards the outlet at Plane 1, 2, 3 and 4.

Table 5.1 Percentage of increment of entrance region with various Re

Re	Entry Length (m)	Increment of velocity magnitude towards entrance region (%)	Increment of Nusselt number with correlation of Re (%)
140	0.0005	2.36	7.16
300	0.0020	4.47	10.2
500	0.0040	11.63	18.48

4.5 Local Temperature Distribution

The temperature distribution in x-y plane, namely at the top wall and bottom wall of the microchannel is illustrated in Figure 4.8.

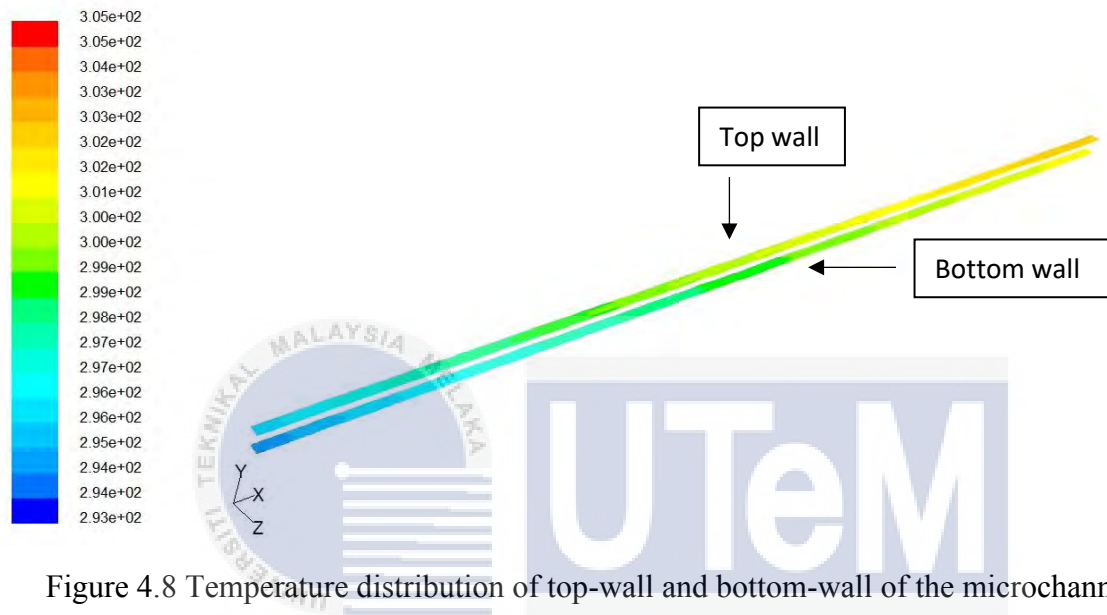


Figure 4.8 Temperature distribution of top-wall and bottom-wall of the microchannel

From the distribution of constant temperature contour lines in Figure 4.8, the temperature gradient decreases along the longitudinal x-direction from the channel inlet to the outlet. The good sign of constant temperature gradient decreases shown the nanofluid flows is in steady along the channel. The small changes of temperature gradient with a linear temperature rise is a good approximation for nanofluid analysis.

In addition, the temperature along the transverse y-direction is constant throughout the channel. The constant temperature contour lines shown that the temperature decreases from the top wall to the bottom wall.

The temperature distributions at two x-z planes, the side wall where $z = W_{w2} = 0.0215\text{mm}$ and the middle plane of the channel, $z = b = 0.05\text{mm}$ are plotted in Figure 4.3a and b, respectively.

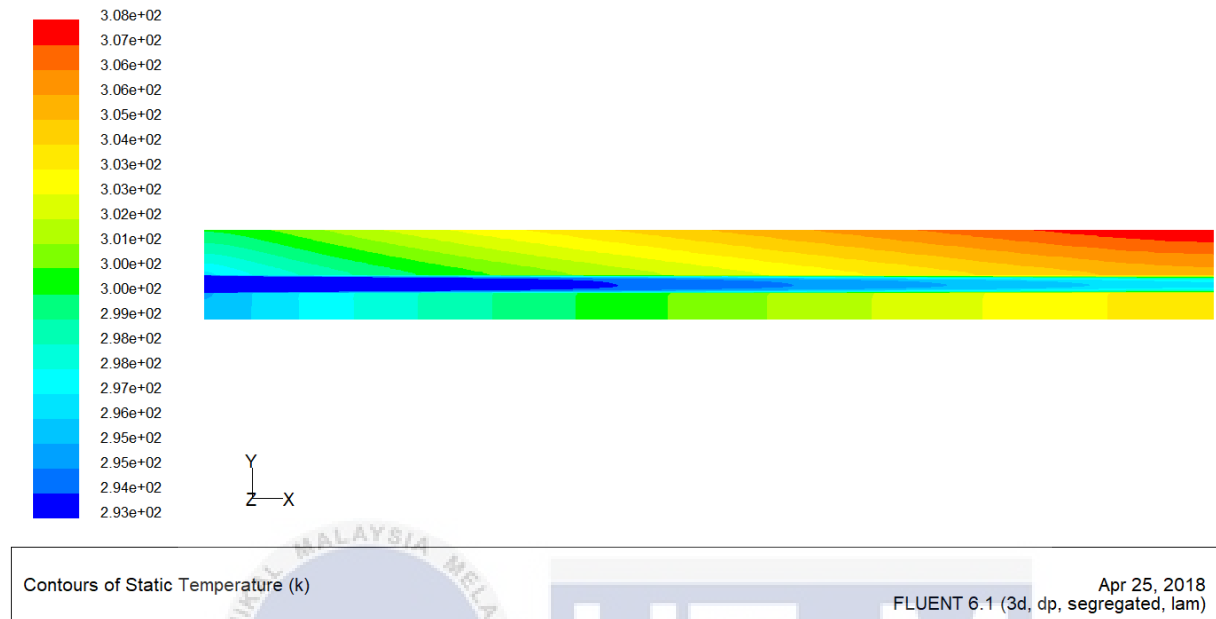


Figure 4.9a) Middle plane heat sink ($z=0.05\text{mm}$)

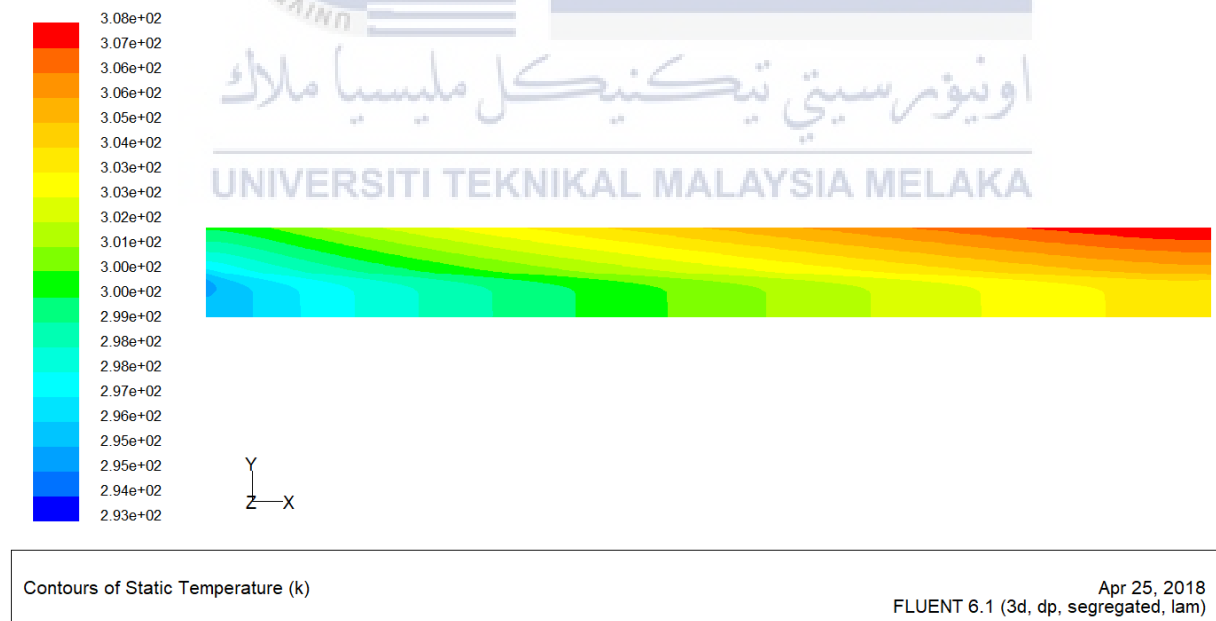


Figure 4.9b) Side plane heat sink ($z=0.0125\text{mm}$)

In Figure 4.9a, the shape of the channel and the temperature distribution is clearly visible due to the large difference in temperature gradient between solid and liquid boundaries. As silicon has high thermal conductivity, the temperature gradient in the silicon is much smaller than alumina nanofluid proving two different regions are analysed as illustrated in both Figures 4.9a and b, respectively.

The location of the channel can be seen at the central of the microchannel and the constant temperature contour lines are similar in the solid region as in Figure 4.9a and b. This proved that the temperature is nearly constant along the transverse y-direction in the solid region. It can also be noticed that from Figure 4.9a and b, the temperature gradient along the z-direction in the solid region above the channel is larger than the region below the channel at a given longitudinal distance x.

The temperature gradient at y-z directions in the solid region below the channel is so small it can be regarded as isothermal where it shown that the selection of material and thickness of solid region above the channel is crucial for the best performance of heat transport in microchannel.

Constant heat flux supplied with adiabatic solid boundary has low temperature at the inlet and increasing linearly towards the outlet as in Figure 4.10. Higher Reynolds number has low temperature distribution in which is good approximation for microchannel cooling application.

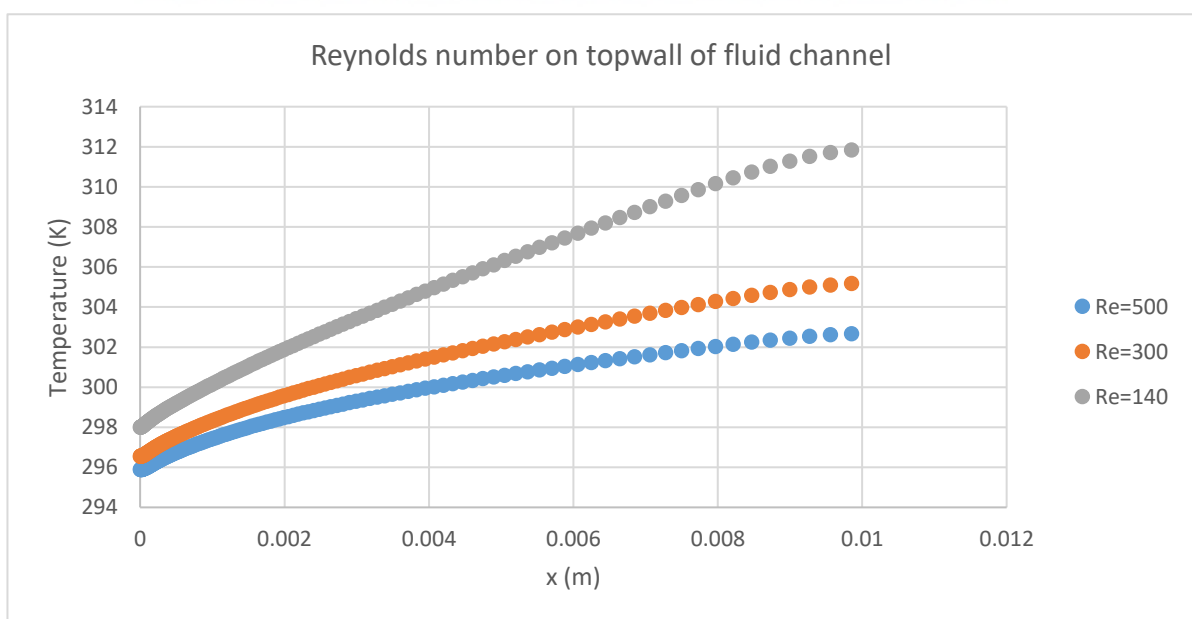


Figure 4.10 Reynolds number on top wall of fluid channel

4.6 Heat Flux

Several Reynolds number of 140, 300 and 500 is used in the studies in simulating the nanofluid flows inside the microchannel. Different Reynolds number provides different correlation to the nanofluid flows as the flows be affected by fluid velocity, thus affecting the Nusselt number.

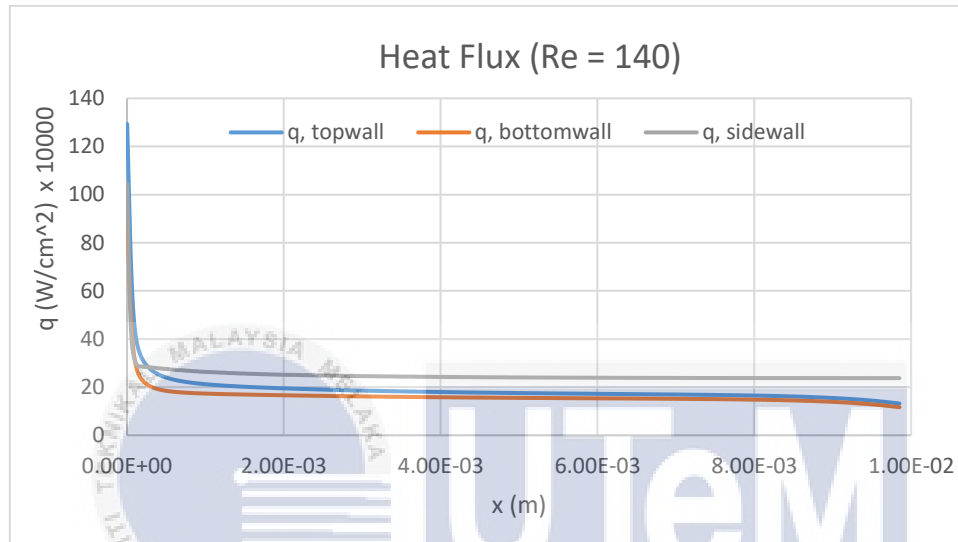


Figure 4.11a) Heat flux of Re =140 at channel fluid contact region

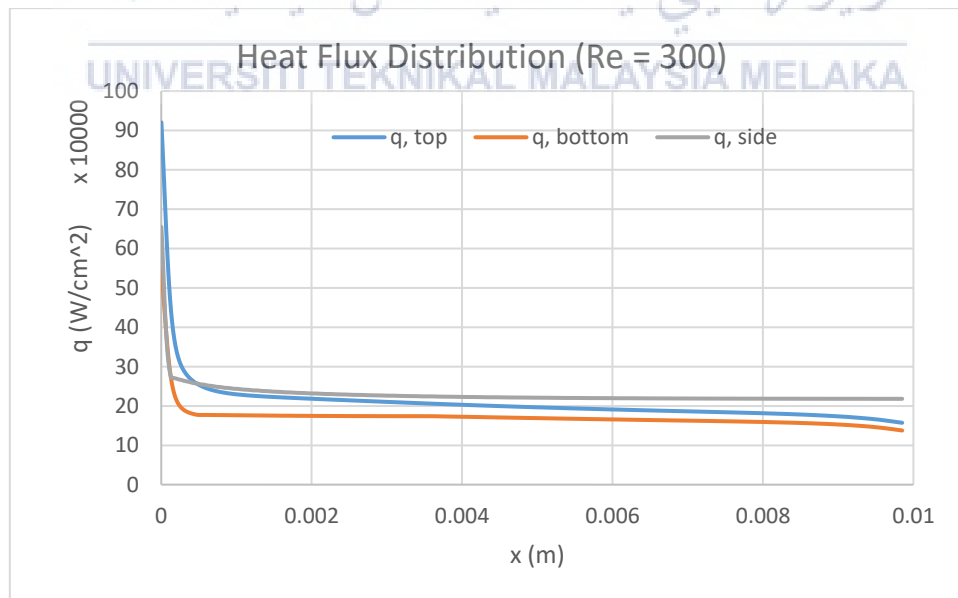


Figure 4.11b) Heat flux of Re = 300 at channel fluid contact region.

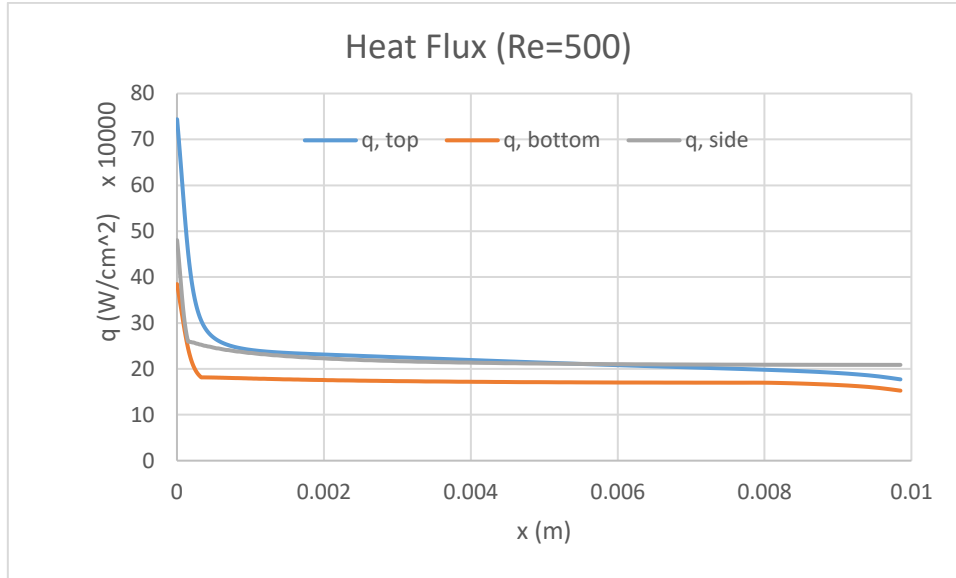


Figure 4.11c) Heat flux of Re = 500 at channel fluid contact region

Furthermore, Figure 4.11a, b and c as above shown the heat flux distribution along the contact region between solid and fluid. The higher heat flux means that there is more quantity of heat entering the fluid particles thus help in cooling the solid region. Based on Figure 4.11, the heat flux distribution along the x-direction is nearly constant for top, bottom and sidewall for every Reynolds as the flow is fully developed.

Comparing the result of top wall and bottom wall of the nanofluid channel, the heat flux of the top wall is slightly larger than at the bottom wall. It shown that the heat supplied is spread out very effectively within the solid region from the top wall by conduction. Even so, the heat flux at the side wall is higher than both top wall and bottom wall due to short distance between the channel side walls and the large velocity gradient presented.

Comparing the Reynolds number to the heat flux distribution shown based on Figure 4.11c, Reynolds number of 500 has the largest deviation of heat flux at the side wall compared to others Reynolds. The largest deviation shown that the heat produced from the heater to the side wall are evenly distributed with the perfect meshed condition.

4.7 Nusselt Number

The effectiveness of heat transfer from solid into the liquid can be understood with correlation of Nusselt number to the distance of longitudinal length, x as plotted in Figure 4.12 below.

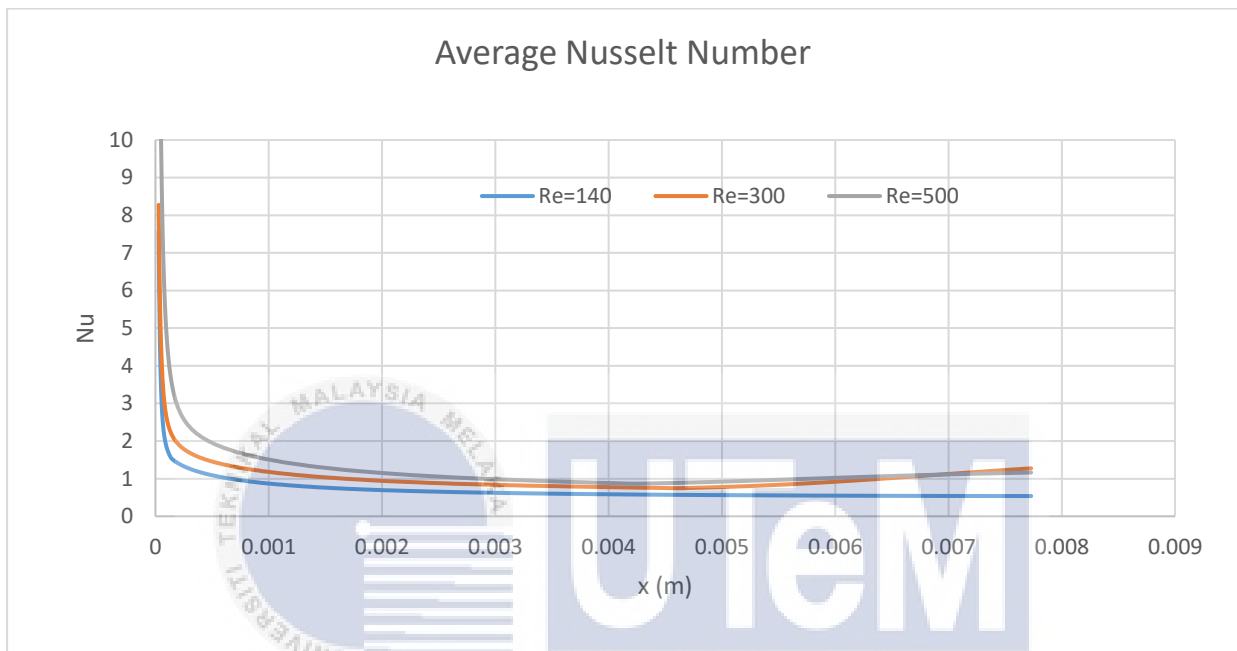


Figure 4.12 Comparison of average Nusselt number

Based on Figure 4.12, higher Reynolds presented higher Nusselt number due to different inlet velocity. The Nusselt number distribution is high value at the entrance region and lower value near the channel outlet. The Nusselt number distributions at the channel top and bottom walls are essentially identical. The Nusselt number at the side wall is symmetrical about the middle plane, which is different from the corresponding heat flux distribution. This is due to channel geometry and flow conditions that attributes to the value of Nusselt number.

CHAPTER 5

Conclusion

5.1 Introduction

The results and discussions of this study will be concluded and summarized in this chapter. Several assumptions have been identified as boundary condition set for present studies as mentioned in methodology section. The velocity profiles and simulation of nanofluid flows will also be stated in this chapter.

5.2 Conclusion

The major objectives of the present studies are to simulate the nanofluid flows and investigate the velocity profiles at various Reynolds. Nanofluid flows show a good approximation of contour lines in $x - y$ plane from top wall to bottom wall where the temperature gradient decreased along longitudinal $x -$ direction from inlet to outlet in steady motion as in Figure 4.8. The numerical results of present studies also show the temperature distribution in the solid region along the transverse $y -$ direction is nearly constant and clearly visible due to large difference in temperature gradient between solid and liquid boundaries as shown in Figure 4.9. Flow in the channel is laminar and fully developed flow with the used of low Reynolds number of 140, 300 and 500 in which results to relatively short entrance region. Temperature rise along the flow direction of nanofluid flows in the solid and liquid regions can be approximated as linear. The highest temperature point is above the channel outlet, which is located at the heated base surface of the heat sink.

Higher values of heat flux and Nusselt number are obtained at the channel inlet and approached to zero in channel outlet. Increasing Reynolds number increases the velocity magnitude together with the length of developing region and the effect become more pronounced at high Reynolds number as indicated in Figure 4.5. Reducing the temperature of

the heated base surface of the heat sink, especially near the channel outlet increases the thermal conductivity of the solid substrate.



References

- Akbarinia, A., Abdolzadeh, M., & Laur, R. (2011). Critical investigation of heat transfer enhancement using nanofluids in microchannels with slip and non-slip flow regimes. *Applied Thermal Engineering*, 31(4), 556–565.
<https://doi.org/10.1016/j.applthermaleng.2010.10.017>
- Bahiraee, M. (2016). Particle migration in nanofluids: A critical review. *International Journal of Thermal Sciences*, 109, 90–113. <https://doi.org/10.1016/j.ijthermalsci.2016.05.033>
- Cengel, Y. A. ., & Cimbala, J. M. . (2014). *Fluid Mechanics: Fundamentals and Applications*. Retrieved from http://highered.mheducation.com/sites/0073380326/information_center_view0/index.html
- Coronella, C. J. (2008). *Handbook of Heat Transfer Calculations* (Vol. 99).
- D.V., G., J., D., & J.P, M. (2014). Heat Transfer and Pressure Drop in Microchannels with Different Inlet Geometries for Laminar and Transitional Flow of Water. *Australian Journal of*, (February), 1–28. Retrieved from [http://www.cdanz.org.nz/files/ajcd/AJCD13\(3\) spring.pdf#page=50](http://www.cdanz.org.nz/files/ajcd/AJCD13(3) spring.pdf#page=50)
- Esionwu-k, C., Marker, A., & Claus, M. (2014). Further Aerodynamics and Propulsion and Computational Techniques CFD Solution Methodology, (march).
- Jung, J. Y., Oh, H. S., & Kwak, H. Y. (2009). Forced convective heat transfer of nanofluids in microchannels. *International Journal of Heat and Mass Transfer*, 52(1–2), 466–472.
<https://doi.org/10.1016/j.ijheatmasstransfer.2008.03.033>
- Kim, B. (2016). International Journal of Heat and Fluid Flow An experimental study on fully developed laminar flow and heat transfer in rectangular microchannels. *International Journal of Heat and Fluid Flow*, 62, 224–232.
<https://doi.org/10.1016/j.ijheatfluidflow.2016.10.007>
- Osborne, D. G., & Incropera, F. P. (1985). Experimental study of mixed convection heat transfer for transitional and turbulent flow between horizontal, parallel plates. *Hf. J. Hear Mass Trmfer*, 28(7), 1337–1344. [https://doi.org/10.1016/0017-9310\(85\)90164-4](https://doi.org/10.1016/0017-9310(85)90164-4)
- Peiyi, W., & Little, W. A. (1983). Measurement of friction factors for the flow of gases in very fine channels used for microminiature Joule-Thomson refrigerators. *Cryogenics*, 23(5), 273–277. [https://doi.org/10.1016/0011-2275\(83\)90150-9](https://doi.org/10.1016/0011-2275(83)90150-9)
- Qu, W., & Mudawar, I. (2002). Analysis of three-dimensional heat transfer in micro-channel heat sinks. *International Journal of Heat and Mass Transfer*, 45(19), 3973–3985.
[https://doi.org/https://doi.org/10.1016/S0017-9310\(02\)00101-1](https://doi.org/https://doi.org/10.1016/S0017-9310(02)00101-1)
- ŞİMŞEK, E. (2016). EXPERIMENTAL INVESTIGATION OF NANOFLUID BEHAVIOR IN MICROCHANNELS, (June).
- Vegad, M., Satadia, S., Pradip, P., Chirag, P., & Bhargav, P. (2014). Heat transfer characteristics of low Reynolds number flow of nanofluid around a. *Procedia*

Technology, 14(1), 348–356. <https://doi.org/10.1016/j.protcy.2014.08.045>

Zhang, H., Shao, S., Xu, H., & Tian, C. (2013). Heat transfer and flow features of Al₂O₃-water nanofluids flowing through a circular microchannel - Experimental results and correlations. *Applied Thermal Engineering*, 61(2), 86–92.

<https://doi.org/10.1016/j.applthermaleng.2013.07.026>

Zhang, X., He, F., Hao, P., Gao, Y., Sun, L., Wang, X., & Jin, X. (2016). Characteristics of Liquid Flow in Microchannels at very Low Reynolds Numbers. *Chemical Engineering & Technology*, 39(8), 1425–1430. <https://doi.org/10.1002/ceat.201500743>

